Proceedings of the 17th Pan-American Conference on Soil Mechanics and Geotechnical Engineering (XVII PCSMGE), and 2nd Latin-American Regional Conference of the International Association for Engineering Geology and the Environment (IAEG), La Serena Chile, 2024.

Construction, execution, and interpretation of compression static load test on 48 m depth piles at Puerto Vallarta

Construcción, ejecución e interpretación de pruebas de carga estáticas, de compresión, en pilas de cimentación a 48m de profundidad en Puerto Vallarta, México.

Nallely Flores, Guillermo Clavellina, Sergio Villar, Uriel Rodriguez.
Engineering Department, CIMESA, Soletanche-Bachy México.

ABSTRACT: This paper describes all activities carried out from two static compression load test on piles of 37.5 and 48.0 m depth at an important project in Puerto Vallarta, México, including construction, test execution, interpretation of results of the load test and calibration results by 3D Finite Elements Models. The insight provided by these experiences contribute to get better understanding of the soils at this region of México and confirm the design of the foundation of this important project.

KEYWORDS: compression load, depth foundation, finite elements

1 INTRODUCTION.

The project involves construction of two buildings at Puerto Vallarta, Jalisco, México.

The objective of the execution of compression static load test on piles (0.8m diameter and 37.5 and 48.0 m depth) was to confirm the bearing capacity of the piles considered as foundation. These tests were conducted at different depths within predominantly alluvial soil strata. The lateral loads of the project reached 700 t, which required the construction of rectangular piles (barrettes). This approach involved orienting the side with greater inertia in the direction of application of the load.

The cost of the test pile is more expensive for a barrette than a circular pile. However, the results of a circular load test were taken and extrapolated to the section of the barrettes across the 3D finite element model.

Finally, the foundation was designed with extrapolation results.

2 STRATIGRAPHY

The geotechnical model shown in Table 1 was defined according to different geotechnical studies carried out for the project. The mechanical properties of silts and clays were obtained by UU triaxial test, while the properties of sands were determined through phicometer tests.

Table 1. Geotechnical model

Geotechnical unit	Depth From (m)	Until (m)	γ (t/m^3)	c (t/m^2)	φ (°)	E (t/m^2)
U1	0.0	-2.4	1.97	4.4	21	380
U2	-2.4	-28.0	1.84	6.7	00	475
U3	-28.0	-35.0	1.94	7.7	23	1200
U4	-35.0	-40.0	2.00	6.0	35	2500
U5	-40.0	-44.0	1.81	14.3	00	520
U6	-44.0	-48.0	2.00	6.0	37	3000

Where:

U1	Superficial layer
U2	Clay and silt intercalations
U3	Sand and Silt intercalations
U4	Alluvial soils
U5	Clay and Silt layer
U6	Alluvial soils
γ	Volumetric weight
c	Soil cohesion
ϕ	Soil friction angle
E	Soil elastic modulus

Is important to recognize that units 4 and 6 are part of the same soil formation. Between the soils mentioned above (Unit 5) there is a clay layer with a low modulus of elasticity. It is only 4.0 m thick.

The groundwater laver was found at -2.7 m.

3 CALCULATION OF BEARING CAPACITY

3.1 *Theorical axial load capacity*

The axial compression load capacity of the 0.80 m diameter piles was calculated at depths of 37.5 and 48.0 m, in accordance with the Complementary Technical Standards for Design and Construction of Foundation for Mexico City (RCCDMX).

$$\sum Q\ F_c < R$$

$$R = C_p + C_f$$

$$C_p = \left(P'_v\ N^*_q\ F_R + P_v\right)A_p$$

$$N^*_q = N_{min} + L_e\left(\frac{N_{max}-N_{min}}{4\,B\,\tan 45°+{}^{\varphi}/_{2}}\right),\ \text{if}\ \ {}^{L_e}/_{B} \le 4\,\tan(45° + {}^{\varphi}/_{2})$$

$$N_q^* = N_{max}, \text{ if } {}^{L_e}/_{B} > 4\tan(45° + {}^{\varphi}/_{2})$$

$$C_f = P_p * F_R * \sum P_v' * \beta_i * L_i$$

$$\beta_i = 1.5 - 0.24 * \sqrt{Z_i} \qquad 0.25 \leq \beta \leq 1.20$$

Where:

$\sum Q\ F_c$ vertical actions affected by its respective load factor.
A Area of foundation element
R is the reduced unit load capacity.
C_p Cross sectional area of pile
N_q^* Load capacity coefficient
N_{min} Minimum load capacity coefficient
N_{max} Maximum load capacity coefficient
L_e Length of pile embedded in the frictional layer.
F_R Resistance factor, taken 0.35
B Diameter of the pile
P_v Total vertical pressure due to the weight of the soil at depth of the pile
P_v' Effective vertical pressure due to the weight of the soil at depth of the pile

Table 2. Bearing capacity calculations

Depth Foundation	Cf (t)	Cp (t)	Ct (t)
37.50	492	532	1024
48.00	608	683	1292

According to ASTM -D1143 standard, the test loads for piles at -37.5m and -48.0m where:

Table 3. Load test

Pile ID	Df (m)	Q test (t)
PP-1	37.50	1,600
PP-2	48.00	1,900

3.1 *Theorical Lateral Load Capacity*

The lateral load capacity was calculated using the program "Picasso" from Soletanche Bachy Group, which is based on the calculation methodology of the NF P94 262 Standard.

This theory considers the modeling of deep foundations based on Menard pressuremeter tests, which are used to construct a stress-displacement curve. The theory is applicable to one pile or a group of foundation elements.

$$K_f = \frac{12E_M}{\frac{3B_0}{4B}\left[2.65\frac{B}{B_0}\right]^{\propto} + \propto} \quad \text{If } B \geq 0.60$$

$$K_f = \frac{12E_M}{\frac{3}{4}[2.65]^{\propto} + \propto} \quad \text{If } B < 0.60$$

$$K_s = K_f$$

$$r_f = \frac{BP_L}{1.7}$$

$$r_s = 2L_s q_s$$

Where:

K_f is linear module to mobilize the pile.
E_M is Menard´s presiometer module.
$\propto$ is soil´s characteristic coefficient obtained by the pressuremeter method.
P_L is a limit pressure.

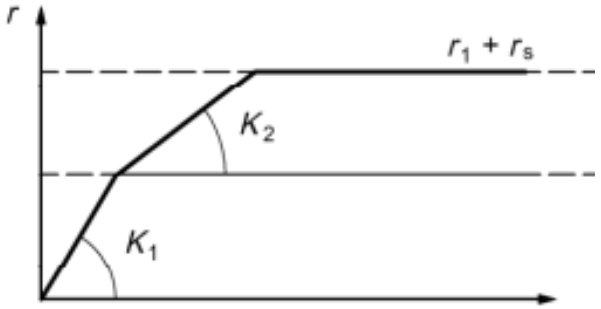

Figure 1. Law of interaction for a lateral load to time.

Picasso models were created to simulate a lateral load test on circular and rectangular elements at a depth of 48m. For the barrettes, loads were applied longitudinally and transversely to understand the behavior in both directions. From these graphs, the lateral load capacity of each element was determined, considering maximum lateral deformations of 1 inch.

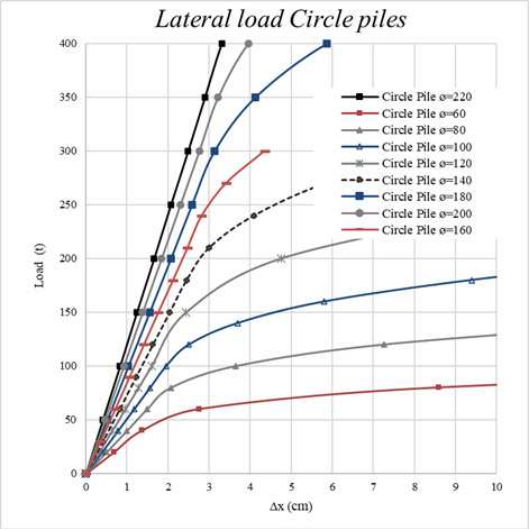

Figure 2 . Graphs Load-deformation (Picasso) for circle piles.

The results of analyses indicated that the lateral load of a 0.60 thick barrette is equivalent to that of a circular pile of 2.0m diameter (deformation of 2.5 cm).
It is therefore important to note that there is a significant difference in volume between solutions with circular piles and barrettes. In fact, the solution with circular piles represents a 30% increase in volume compared to the barrette solution.

It is important to mention that the first layers provide less lateral resistance, so the displacement is governed by the cross section of the foundation element.

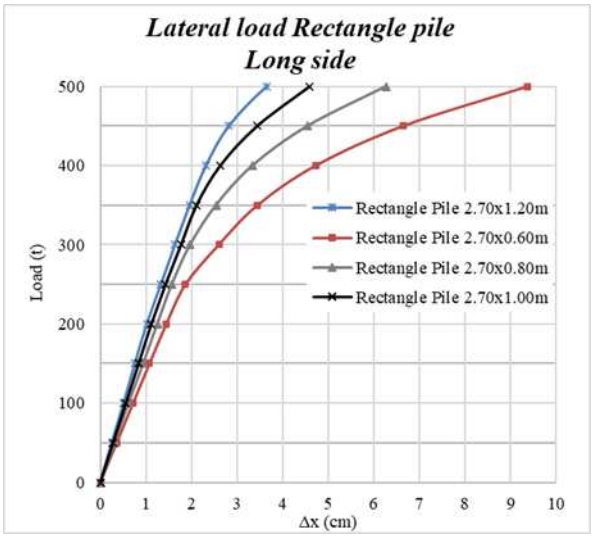

Figure 3 . Load-deformation Graphs (Picasso) for rectangle piles at long side.

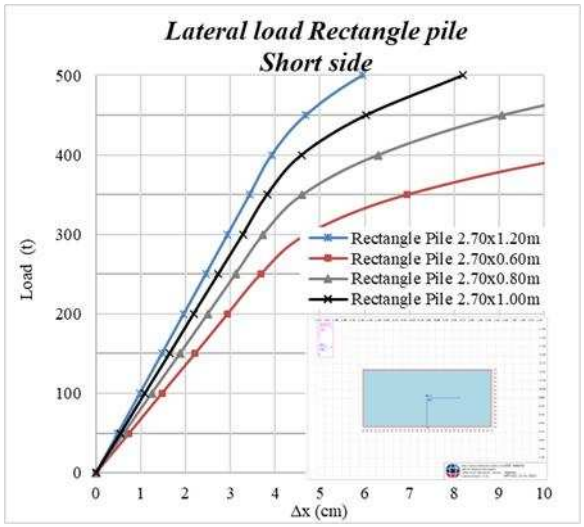

Figure 4 . Load-deformation Graphs (Picasso) for rectangle piles at short side.

4 TESTING AND REACTION PILES

Six reaction piles were constructed, with a distance of 4.70 m between them and the test piles (2). All circular piles had a diameter of 0.80 m, at a depth of 48.0 m. The concrete compression strength was 350 kg/cm^2.

The excavation was stabilized with bentonite slurry, and vertical control of the piles was carried out using the large side auger with topographical control, and additionally, test was conducted with the Koden equipment.

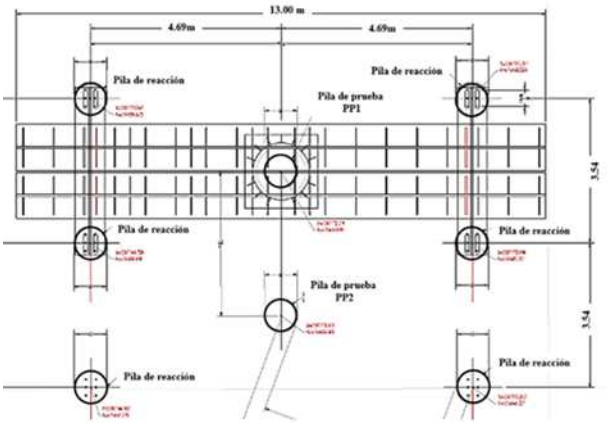

Figure 5 . Geometric locations of test and reaction piles.

Figure 6. Drilling test and reaction piles.

5 REACTION AND INSTRUMENTATION SISTEM

5.1 *Instrumentation*

To verify the load distribution along the test piles, “sister-bars” (strain gages) were installed along pile. The levels strain gages coincide with the layers of the geotechnical model. To quantify the load at the head of the test piles, were installed vibrating wire load cell, with a capacity of 800 t, below of 3 jacks for load application.

5.2 *Reaction frame*

The reaction frames consisted of 3 steel beams with an I section, they joined to the reaction piles by the pre-stressed bars.

Figure 7. Reaction frame

5.3 *Instrumentation frame*

The instrumentation frame consisting of a frames steel beams supported on the ground, the support points should be sufficiently far from the test and reaction piles. Were installed counterweights, deformation gauges (micrometers) and the monitor the settlement of the head of the piles.

Figure 8. Instrumentation at the heat pile.

6 LOAD TEST PROCEDURE

Load tests were executed 30 days after the piles were constructed, the test procedure was following procedure A of ASTM D1143 standard.

This procedure consisted in applying increments of 5% of the maximum test load (increments of 95 and 60 t), each increment lasting 15 minutes, the load and displacement were measured at 0,2,5,10 and 15 minutes after the application of the load. The last increment was maintained for 2 hours to study the behavior during sustained load. Last displacements were measured at 0,5, 10, 20, 30, 45, 60, 75, 90, 105 and 120 minutes.

Two hours later, the load could be reduced of 10% of the maximum applied load, every 15 minutes.

7 LOAD TEST RESULTS

7.1 *Load-Deformation graphs*

Test pile PP-1 (37.5 m depth) reached a maximum load of 1039 t with a vertical displacement of 127mm. Linear elastic behavior was observed up to 650 t, this resistance was taken by the skin friction. Then, the slope of the curve changes, and displacements increase. The behavior indicates that after of 650 t, the load begins to be taken at the tip of the pile.

Test pile PP-2 (48 m depth) reached a load of 1627 t with a vertical displacement of 126mm. Linear elastic behavior was observed up to 945 t. Similar to PP-1, the behavior indicated same slope.

In Figure 10, it can be observed that the first segment of the load-displacement curves of both tests has very similar slope. In the second segment, there is a slight variation in slope, which reflect that the clay layer contributes significantly to the displacement obtained in test pile PP-1

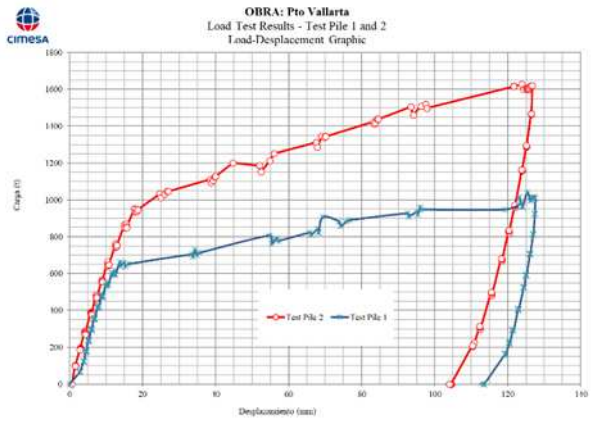

Figure 9. Load-Displacement Graph of pile PP-1 and PP-2.

7.2 *Load-Depth graphs*

The construction of graphs has been realized with the incremental stiffness and tangential modulus method (ASCE,2020). This method takes the products of the mechanical properties of the pile (EA) to define, through micro-deformations at each instrumentation level, a trend line that defines the general behavior at all instrumentation levels and define load each instrument.

The Load-Depth graphs allow understanding the stress distribution along the piles to verify the behavior of the skin friction and the load tip of the pile.

In the graph of test pile PP-1, it can be observed that from 650 t, the slope of the curve changes.

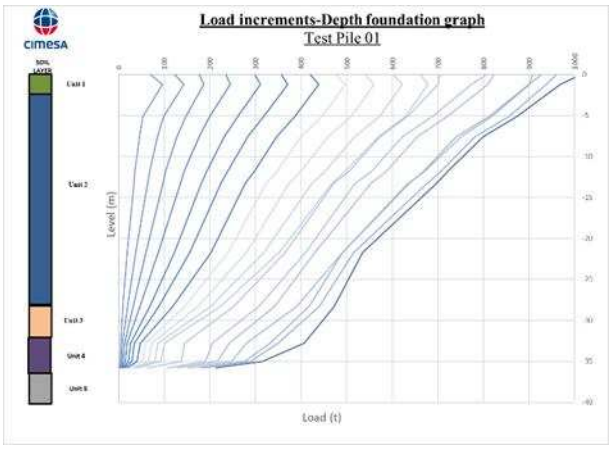

Figure 10. Load-Depth graph PP-1.

In the graph of test pile PP-2, it can be observed that from 945 t, the slope of the curve changes.

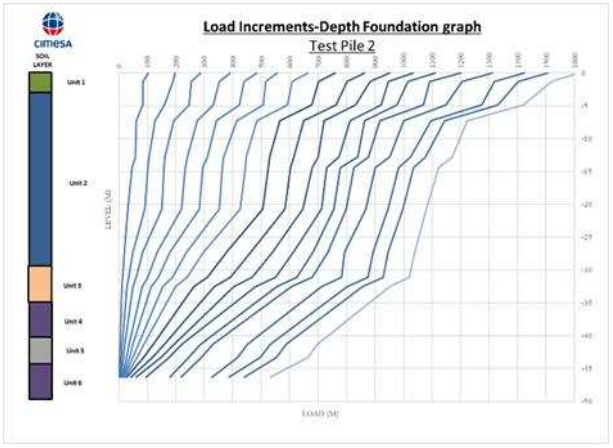

Figure 11. Load Depth graph PP-2.

7.3 *Stresses-displacements graphs by layer soils*

The friction stress graphs per each soil layer were obtained in the same way, using the incremental stiffness method. It shows the stress in each layer and allows the calibration of the parameters used to calculate the initial load capacities.

Cohesion and friction angle were calibrated with friction stress graphs.

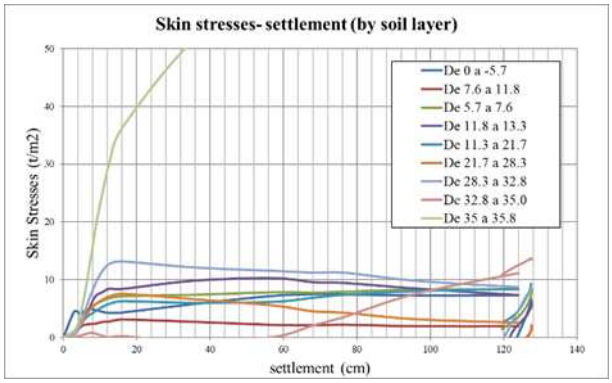

Figure 12. friction Stresses.

8 GEOTHECNICAL PARAMETERS CALIBRATION

According to the results obtained in the load test, realized a calibration of mechanicals parameters to obtain the ultimate load capacity. The calibration results were as follows:

Table 4. Geotechnical model calibrated with load test.

Unit Geotechnic	Depth De (m)	Depth A (m)	γ (t/m^3)	c (t/m^2)	φ (°)	E (t/m^2)
U1	0.0	-2.4	1.85	4.0	21	380
U2	-2.4	-28.0	1.81	6.0	00	475
U3	-28.0	-35.0	1.92	7.0	23	1200
U4	-35.0	-40.0	1.96	0.0	28	2500
U5	-40.0	-44.0	1.70	7.0	00	520
U6	-44.0	-48.0	1.96	0.0	28	3000

From Tables 1 and 4 the mechanical parameters of units 1,2,3, and 5 initially estimated, are slightly different from the calibrated parameter. However, the parameters estimated with the phicometer test, where the tip is embedded (in the alluvial layer) were significantly reduced, from a friction angle with a value of 37° to one of 28°. This does not mean that the internal friction angle was overestimated, but rather that this value is very optimistic for a level of allowable deformations.

Table 5. Calculation of ultimate load capacity with calibrated parameters.

Depth Foundation	Qf ult (t)	Qp ult (t)	Qt ult (t)
37.50	650	389	1039
48.00	945	682	1627

9 EXTRAPOLATIONS OF RESULTS FOR RECTANGULAR PILES

As mentioned above, the foundation of the project was constructed using rectangle piles with a thickness of 60 to 120 cm. In order to confirm the load capacities in a rectangle pile in all section, the first step was to create a 3D finite elements model that represented the load tests results.

This first model considered a circle pile of 80 cm diameter and 48 m length. The soil was represented by the Morh Couloumb constitutive model, which successfully represented the elastoplastic behavior of the soil, with the calibrated parameters found in the previous chapter.

Additionally, an interface was represented with the previously calibrated values of cohesion and skin friction, therefore the R factor was equal to 1. The normal and tangential values (Kn y Kt) were calibrated with the elastic modulus from laboratory test and the deformation results obtained in the load test.

$$K_t = \frac{G_i}{t_v}$$
$$K_n = \frac{E_i}{t_v}$$

Were:
$K_t =$
$K_n =$
$t_v = virtual\ tickness\ factor$
$R = Strength\ Reduction\ Factor$

The general mesh was modeled as a solid of 20x20x70m, and it was discretized into elements of 2.0, 1.0 and 0.20m.

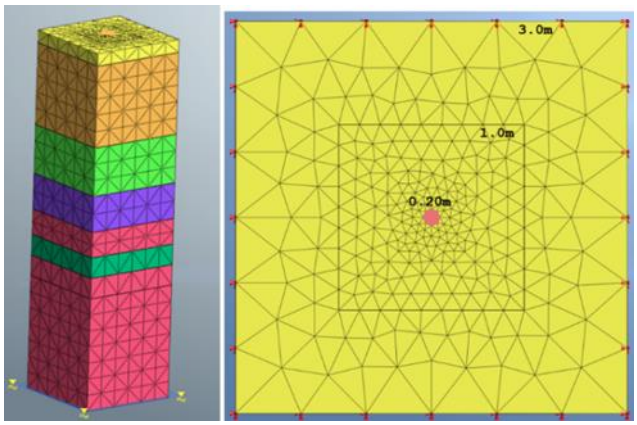

Figure 13. Finite Element Mesh for circle pile model

The stages of analysis considered were as follows:

- Initial conditions
- Pile construction: the properties of the soils were changed to concrete properties, and previously defined interfaced was activated.
- Load increments: constant increments, ranging from 200 t to 1,600 t

As illustrated in Figure 14, the results of the 3D model align with the findings of the load test conducted on test pile PP-2.

In the same model, calibration for lateral load was performed using the information previously calculated in the Picasso models, ensuring that the axial load capacity obtained in the initial calibration was not affected.

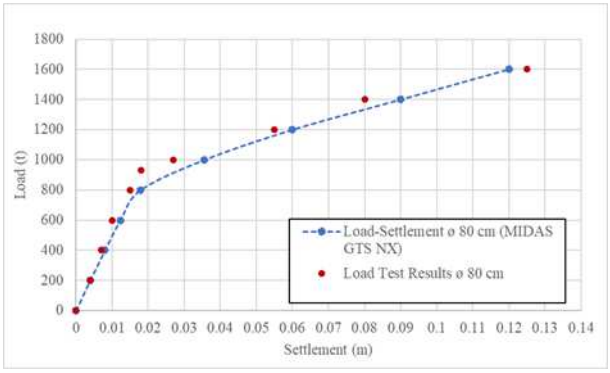

Figure 14. Comparation of Load-Deformation graphs with results of element finite model

In the graphs, it can be observed that the behavior in the Load-Displacement curve of the circular pile under lateral load in the 3D model is the same as that obtained analytically. At this displacement, it is observed in the curve that the load is practically the same.

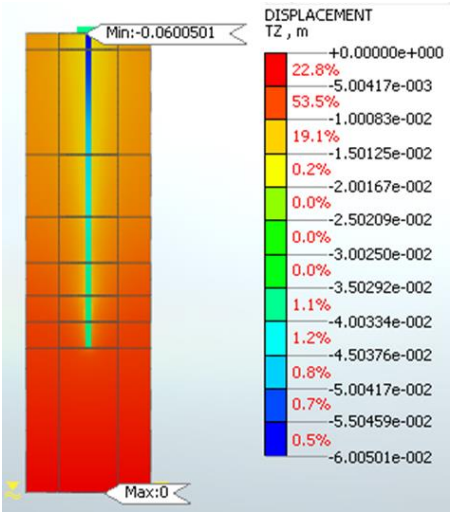

Figure 15. Displacement in finite elements model

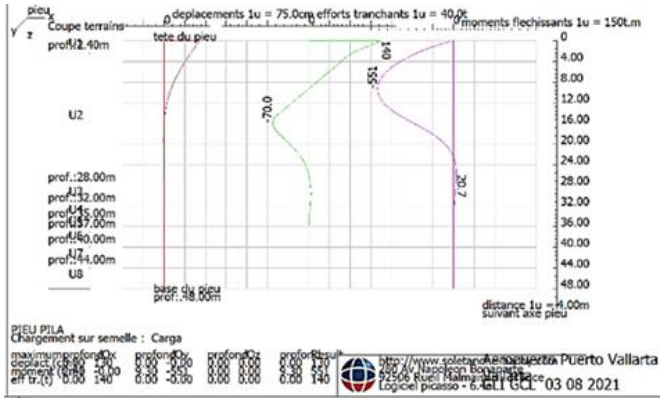

Figure 15. Typical results of lateral load model in Picasso

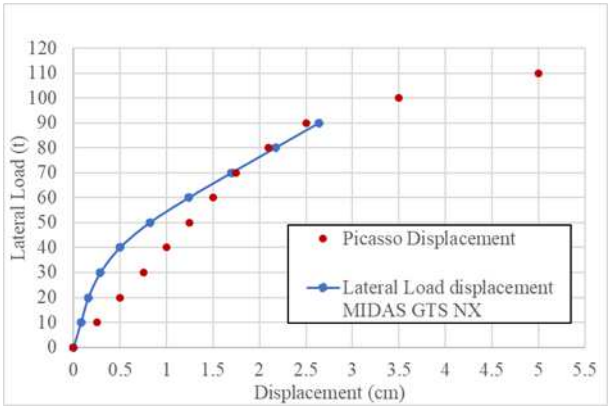

Figure 16. Results of calibration of circle pile with finite elements model (lateral load)

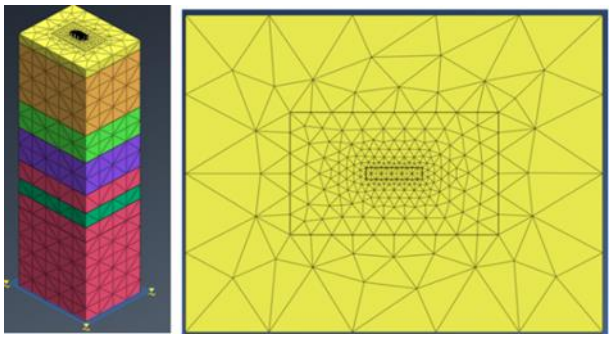

Figure 17 Finite Element Mesh for rectangle pile model

Using all calibrated parameters in the circular pile model, a model for rectangular pile was made.

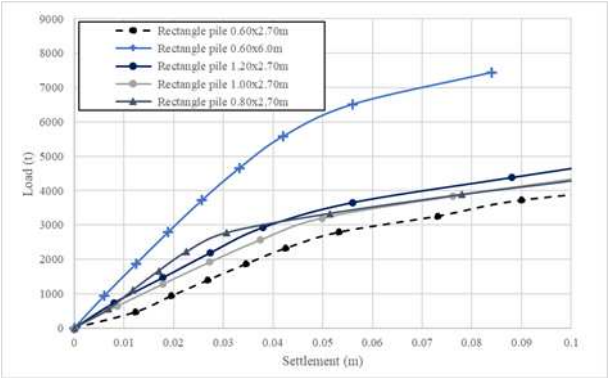

Figure 18. Load-Displacement graph obtained of EFM 3D for rectangle piles (axial loads)

The lateral load curves from the 3D finite element models in rectangular piles show a similar behavior to the data obtained from the Picasso program calculations. The difference between the FEM and Picasso results is in the range of 50 t for lateral displacements of less than 5 cm. Therefore, the predictions are in good correlation and approximation.

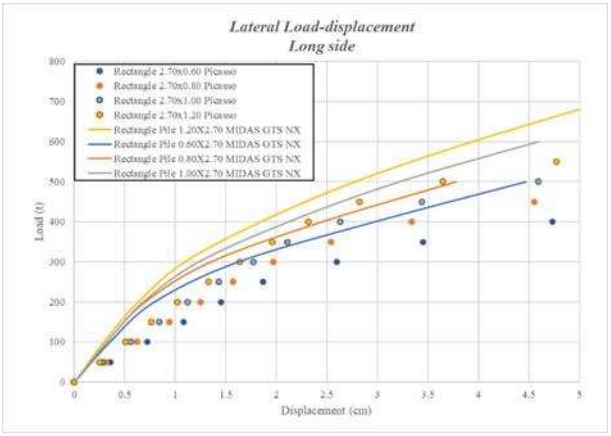

Figure 19. Load-Displacement graph obtained of EFM 3D for rectangle piles (lateral loads in short side)

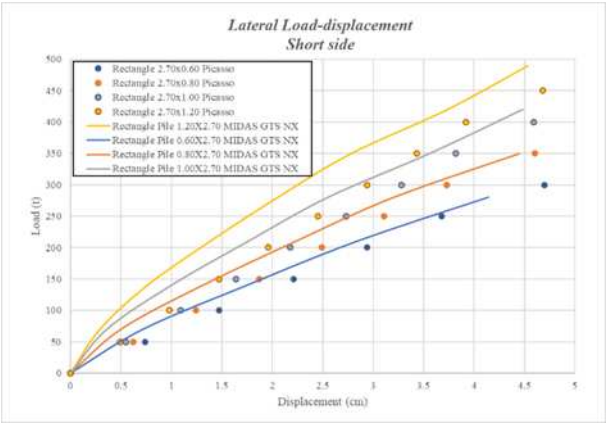

Figure 20. Load-Displacement graph obtained of EFM 3D for rectangle piles (lateral loads in long side)

9 CONCLUSIONS

The skin friction on the pile was conservatively estimated to be 5 t/m², while in the load test it was confirmed that it operates at stresses of around 7-8 t/m². Regarding the tip stress, it is evident that the intermediate clay stratum (U5) contributes significantly to increase deformations in the piles at a depth of 37.50 m, resulting in a reduction in their load capacity from 1064 t/m^2 to 778 t/m^2. The bearing load capacity for the piles installed at 48 m was confirmed by the load test.

The execution of load tests is an effective method for confirming the load-bearing capacity and the depth of foundation elements. Three-dimensional numerical modeling tools permit the extrapolation of results from load tests on elements of different geometries to others with a high degree of reliability and practicality.

Nevertheless, the execution of load tests on deep foundation elements at scale and with real geometries should not be replaced.

In fact, it is always recommended above theoretical estimates and numerical modeling.

The theory used from the NF P94 262 standard was verified to approximate good results with the calibrated parameters.

10 REFERENCES

- ASTM D1143, (2020). “Standard Test Methods For Deep Foundation Under Static Compressive Load”
- Gobierno De La Ciudad De México, (2017) “Reglamento De Construcción Y Normas Técnicas Complementarias para Diseño y Construcción de Cimentaciones”
- NF P 94 262, Normes d'application nationale de 'Eurocode 7 - Fondations profondes
- TGC, (2021), Recomendaciones Geotécnicas para el Nuevo Edificio Terminal del Aeropuerto de Puerto Vallarta
- TGC, (2021), Nota Técnica No 2 Capacidades de carga y módulos de reacción
- ASCE GeoCongress 2020, Instrumented Static Loading Tests Using the Incremental Rigidity Method Minneapolis.